Supermassive Black Holes and the Evolution of Galaxies *

D. Richstone, E. A. Ajhar, R. Bender, G. Bower, A. Dressler, S. M. Faber, A. V. Filippenko, K. Gebhardt, R. Green, L. C. Ho, J. Kormendy, T. Lauer, J. Magorrian, S. Tremaine

9 October 1998

Black holes, an extreme consequence of the mathematics of General Relativity, have long been suspected of being the prime movers of quasars, which emit more energy than any other objects in the Universe. Recent evidence indicates that supermassive black holes, which are probably quasar remnants, reside at the centers of most galaxies. As our knowledge of the demographics of these relics of a violent earlier Universe improve, we see tantalizing clues that they participated intimately in the formation of galaxies and have strongly influenced their present–day structure.

Black holes are a prediction of Einstein's theory of gravity, foreshadowed by the work of Michell and later Laplace in the late 18th century. K. Schwarzschild discovered the simplest kind of black hole in the first solution of Einstein's equations of General Relativity, and Oppenheimer was among the first to consider the possibility that black holes might actually form in nature. The subject gained life in the 1960s and 70s, when supermassive black holes were implicated as the powerhouses for quasars and stellar–mass black holes were touted as the engines for many galactic X–ray sources. In the last decade, we have progressed from seeking supermassive black holes in only the most energetic astrophysical contexts, to suspecting that they may be routinely present at the centers of galaxies [1, 2, 3].

The defining property of a black hole is its event horizon. Since the horizon itself is invisible, we must often settle for evidence of mass without light. All dynamical techniques for finding supermassive black holes at the centers of galaxies rely on a determination of mass enclosed within a radius r from the velocity v of test particles;

*Almost identical to the text in Nature Oct 1, 1998 in Newtonian physics, this mass is $M_r = \alpha\, v^2 r/G$. Determining α requires a detailed dynamical analysis, but it is often of order 1. In cases where there is extra mass above that associated with starlight, we refer to the object as a "massive dark object" (or MDO). In most of the cases discussed in this paper, it is likely that the MDO is a supermassive black hole (MBH), but in only a few cases have plausible alternatives to a black hole been ruled out. These are important as they establish the reality of MBH and justify the interpretation of less compelling objects as MBHs.

1 Black holes as the energy sources of quasars

Black holes are thought to exist in two mass ranges. Small ones of $\sim 10 M_\odot$ are the evolutionary end points of some massive stars. This paper discusses the much more massive ones that might power quasars and their weaker kin, active galactic nuclei (AGN). Quasars produce luminosities of $L \sim 10^{46}$ ergs/sec ($\sim 10^{12} L_\odot$). Where they power double–lobed radio sources, the minimum energy stored in the lobes is $E \sim 10^{60-64}$ ergs. The mass equivalent of this energy is $M = E/c^2 \sim 10^{6-10} M_\odot$, and the horizon scale associated with that mass is $R_S = GM/c^2 \sim 10^{11-15}$ cm. Although most quasars do not vary much at visual wavelengths, a few objects change their luminosity in minutes at high energies [4, 5]. Since an object cannot causally vary faster than the light–travel time across it, such objects must be smaller than $R \sim c\tau \sim 10^{13}$ cm. Although relativistic corrections can alter this limit somewhat in either direction via Doppler boosting or gravitational redshift, there is no escaping the conclusion that many quasars are prodigiously luminous yet tiny, outshining a galaxy in a volume smaller than the solar system.

The small size together with the enormous energy output of quasars mandates black hole accretion as the energy source. Most investigators believe that quasars and AGNs are MBHs accreting mass from their environment, nearly always at the center of a galaxy [6, 7, 8]. Black holes of mass $> 10^7 M_\odot$ must normally lie at the center because dynamical friction drags them to the bottom of the potential well. This location is now clearly established for low redshift ($z \lesssim 0.3$) quasars [9]. The connection between MBHs and quasars was first made by Zeldovich [10] and Salpeter [11]. Lynden-Bell [12] sharpened the argument by computing the ratio of gravitational energy to nuclear energy

$$\frac{E_g}{E_n} \sim \frac{\epsilon_g\, GM^2/R}{\epsilon_n\, Mc^2} \sim \left(\frac{\epsilon_g}{\epsilon_n}\right)\left(\frac{R_S}{R}\right) \sim 100\epsilon_g, \tag{1}$$

where R_S is the Schwarzschild radius of a black hole of mass M, R is the size of the quasar, and ϵ_g and ϵ_n are gravitational and nuclear energy conversion efficiencies; the last equality follows from the typical astrophysical thermonuclear efficiency of $\sim 1\%$ and the size scale from variability noted above.

Because quasars were populous in the youthful Universe, but have mostly died out, the Universe should be populated with relic black holes whose average mass density ρ_u matches or exceeds the mass–equivalent of the energy density u emitted by them

[13]. The integrated comoving energy density in quasar light (as emitted) is

$$u = \int_0^\infty \int_0^\infty L\Phi(L|z)dL \frac{dt}{dz} dz = 1.3 \times 10^{-15} \text{erg cm}^{-3}, \tag{2}$$

where Φ is the comoving density of quasars of luminosity L, and t is cosmic time. The corresponding present-day mass density for a radiative efficiency ϵ is $\rho_u = u/[\epsilon c^2] = 2 \times 10^5 \left(\frac{0.1}{\epsilon}\right) M_\odot \,\text{Mpc}^{-3}$. This density can be compared to the luminous density in galaxies, $j = 1.1 \times 10^8 \, L_\odot \,\text{Mpc}^{-3}$ [14], to obtain the ratio of the mass in relic MBHs to the light of galaxies:

$$\Upsilon = \frac{\rho_u}{j} = 1.8 \times 10^{-3} \left(\frac{0.1}{\epsilon}\right) \left(\frac{M_\odot}{L_\odot}\right). \tag{3}$$

2 Dynamical evidence for massive black holes

2.1 First steps

The first dynamical evidence for black holes in galactic centers was the 1978 measurement [15] of a rising central velocity dispersion, reaching ~ 400 km s^{-1}, in the giant elliptical galaxy M87. This object is a prime site to prospect for an MBH by virtue of its AGN features — nonthermal radio emission, broad nuclear emission lines, and a "jet" of collimated relativistic particles being ejected from the nucleus. Isotropic models of the stellar kinematics, when combined with photometry, implied an MDO of $5 \times 10^9 M_\odot$. The result was criticized because the data were also matched by a model with *radially anisotropic* stellar orbits and no black hole. Thus, the importance of understanding the stellar orbital structure of the centers of galaxies was obvious at the very beginning, and this subject has developed in parallel with the search for MBHs.

More convincing evidence was found in the 1980s for MDOs in M31 and M32 (the Andromeda galaxy and its satellite), which are nearby and hence observable at high spatial resolution [16, 17]. Rapid rotation near their centers reduces the danger of confusing a central mass with radial orbits, and Schwarzschild's method of loading orbits in a galaxy potential [18, 19] was used to eliminate unphysical models. Modern methods use Schwarzschild's method to fit the entire line–of–sight velocity distribution for axisymmetric models.

The stellar velocity work on M87 was largely vindicated two decades later by the *Hubble Space Telescope (HST)*, which revealed a small gas disk at the center [20, 21]. The gas is plausibly in circular motion, so the MDO mass estimate is straightforward. These and later data provide strong evidence for an MDO of $3 \times 10^9 M_\odot$ [20, 22], a value similar to but slightly smaller than the one derived in [23].

2.2 Two remarkable examples

The work described above revealed strong examples of MDOs but no iron–clad evidence for MBHs. This gap has now been partly closed in two remarkable objects. The mild AGN NGC 4258 was shown [24] to possess a tiny annular gaseous disk near the nucleus, populated by water masers whose Doppler velocities can be observed with exquisite precision. The rotation curve is Keplerian to high accuracy over the annulus width ($0.13 - 0.26\,\mathrm{pc}$). The very small velocity residuals of $\lesssim 1\%$ inspire confidence in the derived mass of $3.6 \times 10^7 M_\odot$ [25]. The extraordinarily high implied density of $> 10^9\ M_\odot \mathrm{pc}^{-3}$ (10^{12} if one takes the limits on departures from Keplerian motion as a constraint on the concentration of the mass) permits the use of astrophysical arguments to rule out most other explanations for the dark mass (see below). This is a firm link from MDOs to MBHs.

The center of our Galaxy holds the second confirmed MBH. Near–infrared observations detect *proper motions* of stars in orbit about the galactic center [26, 27] and indicate a rising stellar velocity dispersion down to distances of 0.01 pc. For the first time stars are being observed to orbit an MDO, year by year, with impressive accuracy that will steadily improve. The density of $> 10^{12}\ M_\odot\ \mathrm{Mpc}^{-3}$ within the resolved region is again extraordinarily high, ruling out most alternatives to an MBH.

In the Galaxy and NGC 4258, the MDOs are almost surely MBHs [25] rather than clusters of smaller masses. A cluster of radius r and total mass M of N self–gravitating point masses will collapse or evaporate on a timescale of a few hundred two–body relaxation times, $t_r = 0.14N\,(r^3/GM)^{1/2}\,[\ln(0.4N)]^{-1}$ (some important caveats were noted in [28]). At a chosen nonrelativistic density, the lifetime of the cluster can be made longer than the age of the Universe by making the point masses sufficiently light (and therefore numerous). In NGC 4258 and the Galaxy, this constraint requires constituents with masses $\lesssim 0.1 M_\odot$. Brown dwarfs and white dwarfs with this mass have large radii and would rapidly collide and merge. Thus the remaining candidate components for cluster models are low–mass black holes or noninteracting elementary particles. However, there is no known way to make $0.1 M_\odot$ black holes, and, since non–interacting elementary particles do not radiate energy efficiently they do not settle into a compact configuration. The cases for black holes in both NGC 4258 and the Galaxy therefore seem very strong. The argument for all of the other MDOs is weaker, but, by analogy and by virtue of the overwhelming circumstantial evidence for MBHs in AGNs they are now the preferred explanation.

2.3 Potential new tools

The techniques above are difficult to apply to galaxies containing AGNs. The bright nucleus renders the stellar absorption lines close to the center nearly invisible, and in many cases the nebular emission lines are influenced by nongravitational forces. Nevertheless, in AGNs that emit broad emission lines originating from gas near the central engine ($\Delta v \gtrsim 10,000$ km s^{-1}), one can attempt to estimate a mass from the average velocity of the gas and the radius of the emitting region. The velocity comes from the widths of the lines, but the radius is harder to measure. It can be estimated either from photoionization models of the gas or by "reverberation mapping." In the latter method, the radius is inferred from the time interval (due to light travel) between fluctuations in the continuum radiation and the changes these induce in the emission lines [29].

Masses obtained from reverberation mapping for nearby Seyfert nuclei range from 10^7 to $10^8 M_\odot$ [30], roughly consistent with (but somewhat smaller than) the dynamical results of the previous section. However, the identifications of line width with orbital velocity and time delay with radius are problematic given the absence of any correlation between line width and radius of the form $v \propto r^{-1/2}$ within the same object. Evidently some essential component of the model is still missing. A proper understanding of this technique would give us a powerful tool for more luminous and distant objects [31].

Recent advances in X–ray astronomy have furnished dramatic new evidence for MBHs in AGNs. It had been known for some time that the X-ray spectra of many AGNs show an iron Kα emission line at a rest energy of 6.4 keV, thought to arise from X–ray fluorescence of cold, neutral material in an accretion disk. Until recently, the available spectral resolution was insufficient to test the predicted line profile, but the *Advanced Satellite for Cosmology and Astrophysics* provided the much–awaited breakthrough in the Seyfert 1 galaxy MCG–6-30-15 [32]. The Kα line exhibits relativistic Doppler motions of nearly 100,000 km s^{-1}, as well as an asymmetric red wing consistent with gravitational redshift. The best–fitting disk has an inner radius of only a few Schwarzschild radii. The Fe Kα line profile has now been seen in many objects [33], and data of better quality may eventually even allow measurement of the spin of the black hole [34, 35].

3 The demographics of supermassive central black holes

We now turn to the questions of the number of MBHs in the Universe. Figure 1 illustrates the relationship between black hole mass and host spheroid luminosity from the data in Table 1 (labeled points). The labeled MDO masses seem to correlate with spheroid luminosity (solid line); the upper limits are also consistent with this relation [2, 36]. However, the number of points is small, and, further progress requires more objects. Few objects at the present time have been studied with the detailed spatial resolution and/or modeling of the labeled points.

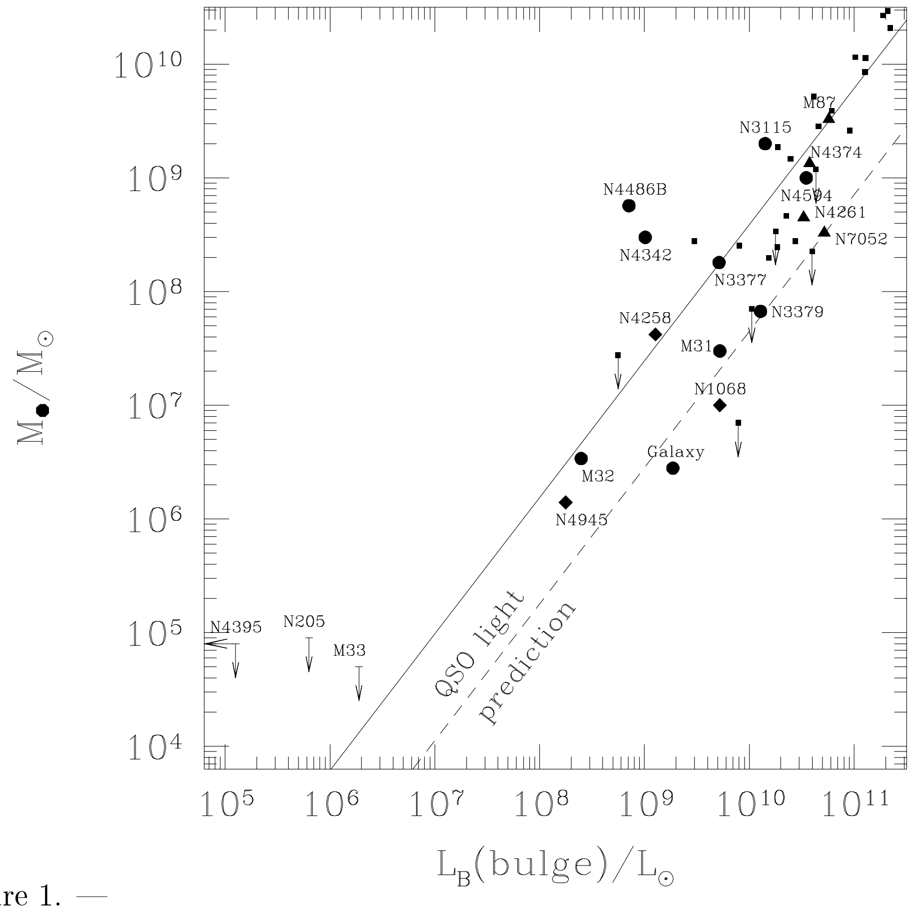

Figure 1. —
Mass estimates of the candidate MBHs in galaxies with dynamical information plotted against the bulge luminosity of their host galaxy. The labeled points are the results of painstaking observation and detailed modelling. The symbols indicate the how $M_\bullet$ was derived: kinematics of gas — triangles; dynamics of stars — filled circles; masers — diamonds; or two-integral modelling using ground-based stellar kinematics — small squares. Arrows indicate upper limits on $M_\bullet$. The solid line is a model with $M_\bullet = 0.005 M_{bulge}$ and . $M_{bulge} = 5(L_{bulge}/10^9 L_\odot)^{1.2}$. The distribution of $M_\bullet$ is roughly Gaussian in $\log(M_\bullet/M_{\rm bulge})$ with mean -2.27 ($M_\bullet/M_{bulge} = 0.005$) and standard deviation 0.5. The dashed line is the quasar light prediction of eqn 3 apportioned according to the bulge mass: $M_\bullet = 2 \times 10^7 (L_{bulge}/5 \times 10^9 L_\odot)^{1.2}$.
The small offset from the observed black-hole/bulge-mass relation indicates that the present integrated density in MBHs is broadly consistent with the integrated luminosity produced by AGNs over the life of the Universe. This offset may reflect a radiative efficiency of average quasar accretion less than 0.10.

DYNAMICALLY IDENTIFIED MDOs

Galaxy	Name	Type	Distance [a] Mpc	M_B Bulge	$M_\bullet$ M_{sun}	Reference
			Stellar Dynamics			
——	Galaxy	Sbc	0.0085	–17.70	2.8×10^6	see [26, 27]
NGC0221	M32	E2	0.7	–15.51	3.4×10^6	[16, 73, 74, 75]
NGC0224	M31	Sb	0.7	–18.82	3.0×10^7	[16, 17]
NGC3115	—	S0	8.4	–19.90	2.0×10^9	[76, 77]
NGC3377	—	E5	9.9	–18.80	1.8×10^8	[78]
NGC3379	M105	E1	9.9	–19.79	6.7×10^7	[79]
NGC4342	IC3256	S0	15.3	–17.04	3.0×10^8	[80]
NGC4486B	—	E1	15.3	–16.65	5.7×10^8	[81]
NGC4594	M104	Sa	9.2	–20.88	1.0×10^9	[81] [82]
			Gas Dynamics			
NGC4374	M84	E1	15.3	–20.96	1.4×10^9	[83]
NGC4486	M87	E0	15.3	–21.42	3.3×10^9	[20, 21]
NGC4261	—	E2	27.4	–20.82	4.5×10^8	[84]
NGC7052	—	E4	58.7	–21.31	3.3×10^8	[85]
			Maser Dynamics			
NGC1068	M77	Sb	15.	–18.82	1.0×10^7	[86]
NGC4258	M106	Sbc	7.5	–17.28	4.2×10^7	[24]
NGC4945	—	Scd	3.7	–15.14	1.4×10^6	[87]
			Upper Limits			
NGC0205	—	Spheroidal	0.72	–9.02	$< 9. \times 10^4$	[88]
NGC0598	M33	Scd	0.795	–10.21	$< 5. \times 10^4$	[89]
NGC4395	—	Sm		–7.27	$< 8. \times 10^4$	[30]

[a] All quantities in this paper are computed for a Friedman-Robertson-Walker Universe with $\Omega = 1$ and $H_0 = 80$ km s^{-1}Mpc^{-1}. Distances to nearby MBHs come from many sources, but are always rescaled to this Hubble constant.

At the risk of greater uncertainty, more galaxies can be included by combining ground–based stellar kinematics with *HST* central light profiles. A simple modeling recipe based on two–integral axisymmetric models has been used on such data for a further 25 E and S0 galaxies [37]. This procedure assumes that the phase–space density is only a function of the energy and one component of angular momentum. MDO masses from this technique can be checked against galaxies with HST spectroscopy. The results for 5 low–mass galaxies with steep inner light profiles show good agreement, but the 2–integral method may overestimate masses by a factor of a few for massive ellipticals like M87, which rotate slowly and have shallow central light profiles. A Bayesian analysis of this sample indicates that MDOs are in fact very common features of normal, bright galaxy centers [37].

All known MDOs with measured masses so far are in galaxies with identifiable spheroidal components, suggesting that black hole formation is *exclusively* linked to spheroid formation. However, several well–imaged low z quasars do not appear to be associated with spheroids [9].

It is clearly important to survey more late–type spirals *without* bulges. So far, we have little *dynamical* evidence on the centers of such galaxies, but AGN activity might perhaps be used as a proxy for a black hole. Seyferts are generally not found in late–type spirals [38], but a single dwarf Seyfert nucleus (out of hundreds surveyed) has been discovered in NGC 4395, a nearby bulgeless Sd IV galaxy The bolometric Seyfert luminosity of this nucleus is 1.4×10^{40} ergs/sec [39], and the Eddington BH mass is only $110 M_{\odot}$, small enough to have been produced by stellar evolution.

There is no evidence for MDOs in low–surface brightness galaxies, although existing studies do not set compelling limits [40].

Our view of these observational results, largely developed over the past decade, is as follows: (i) MBHs are a normal feature of the central regions of bright galaxies, particularly those with spheroids; (ii) their masses scale in rough proportion to host–galaxy spheroid mass; and (iii) the total mass density in black holes is broadly consistent with the mass–equivalent energy density in the quasar light background. We therefore believe that the black hole fossils of the quasar era have been found.

4 Co–evolution of Galaxies and Black Holes

4.1 The Era of Quasars

The improving statistics on local MBHs can be compared to their properties and distribution during the quasar era at $z \sim 3$. Were today's MBHs already fully formed by that time, or was the average MBH smaller then, having grown by later accretion or mergers to form the present population? The evidence is not conclusive but seems to favor some growth.

The epoch of maximal quasar activity in the Universe peaked at the same time, or slightly before, the epoch of maximal star formation, and MBHs must have formed *before* this time to be available to power quasars. Figure 2 illustrates this point by plotting the history of the rate of observed star formation in the Universe [41, 42, 43] together with the density of luminous quasars (those with $L > 3 \times 10^{46}$ ergs/sec, [44]). The rise in starbirth is tracked closely by the rise of luminous quasars. However the bright quasars reach their peak at $z \gtrsim 2$ ($t \leq 1.6 \times 10^{9}$ yr), and then proceed to die off nearly 10^{9} yr before the peak in star formation, which occurs at $z \sim 1.2$ ($t = 2.6 \times 10^{9}$ yr) [45]. The application of extinction corrections to the cosmic star formation rate before $z \sim 2$ is a controversial subject that may evolve rapidly as better IR data become available.

This chronology favors models in which the black hole forms before, or in close asso-

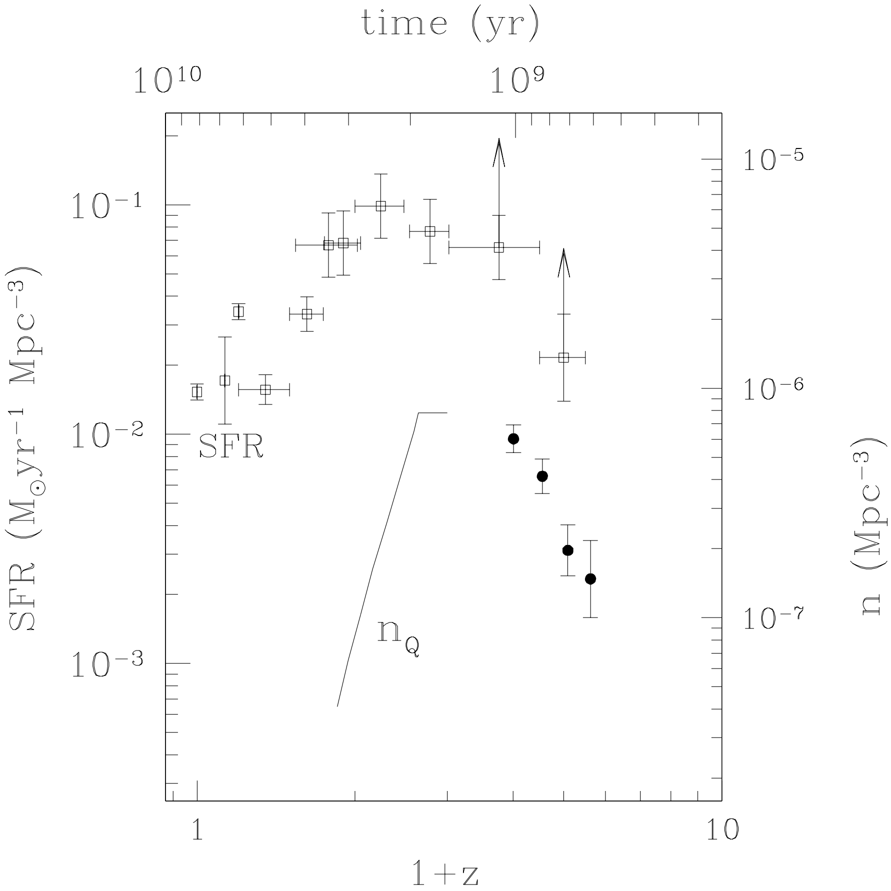

Figure 2. —
A comparison of the density of very bright quasars in the Universe, with the density of star formation, as a function of redshift and cosmic time. The solid line and the filled circles are the comoving number density of quasars (n_Q see [12]) in units of Mpc^{-3}, while the open circles represent estimates of the comoving star formation *rate* (SFR). The SFR can be read off the left axis, and n_Q should be read off the right axis. The arrows on the two highest redshift SFR points indicate an estimate of plausible correction for extinction. The peak of quasar activity in the Universe appears to predate most of the star formation. The times are derived from the redshift assuming $\Omega = 1, H_0 = 80$ km s^{-1}/Mpc.

ciation with, the densest parts of galaxies (for example [46]), as opposed to models in which the galaxy forms first and later spawns the quasar. For this reason we associate the birth of quasars with *spheroid* formation, a process also identified with dense regions that collapse early [47]. The collapse of these regions would predate the average rise of star formation illustrated in Figure 2.

The decline of bright quasars at $z < 2$ seems likely to reflect a loss of fuel. Galaxy mergers, an effective gas transport process, are less frequent as time passes and involve a lower mean density and slower dynamical clock. There is also less gas in galaxies overall (especially spheroids). Radial transport instead may be choked by the onset of chaos, which would make the spheroid axisymmetric [48] or through the creation of an inner Lindblad resonance [49]. Any or all of these effects could play a role in the reduction of fuel for the black hole.

A model in which an MBH forms in every collapsing spheroid invites comparison between the densities of luminous quasars and galaxies at $z \sim 2$, and of fossil MBHs today. To make this comparison, we must identify a quasar of specified luminosity with its fossil MBH mass. We do this under the assumption that the brightest quasars are Eddington–limited, that is, that their luminosity is so great that radiation pressure on nearby electrons balances the gravitational force on associated protons. In this situation, the "Eddington luminosity" is

$$L_E = 1.3 \times 10^{46}\, M_8 \,\text{ergs/sec}, \tag{4}$$

where M_8 is the mass in units of $10^8 M_\odot$.

The comoving density of luminous quasars with $L \geq 6 \times 10^{45}$ ergs/sec reached its peak value of 10^{-6} Mpc^{-3} at $z \sim 3$ [44]. We assume for the moment that the MBHs underlying these bright quasars *have not grown* substantially since then. To estimate the corresponding mass range, we first correct the absolute magnitude limit in the QSO surveys ($M_B < -26.0$, [44, 50]) downward to our H_0 and upward by a bolometric correction factor of 10 [51] to get a lower–limit luminosity of 6×10^{46} ergs/sec. This luminosity implies a MBH mass of $M \sim 4 \times 10^8\, M_\odot$, corresponding to a bulge luminosity of current hosts (from Figure 2) of $\sim 10^{10}\, L_\odot$. Correcting for the total–to–bulge luminosity ratio of 3 [52], and using the luminosity function of bright galaxies [14], we identify the bright quasars of $z \gtrsim 2$ with the half of modern galaxies with $M_B < -20.7$ that have bulges [53], we find a comoving density of such spheroids today of $\rho_G = 10^{-3}\,\text{Mpc}^{-3}$.

Thus, luminous QSO MBHs at $z \sim 3$ are only about 10^{-3} as numerous as their galaxy host descendents today. One way to resolve this discrepancy is to assume that QSOs have very short duty cycles in their bright phase, of order $\eta \sim 10^{-3}$. Since the quasar epoch runs about $t_Q \sim 10^9$ yr from $z \sim 1.5$ to $z \sim 3.5$ (the FWHM of the quasar plot in Figure 2), the lifetime in the bright phase would then be only $t_{up} \sim \eta t_Q = 10^6$ yr. The fractional mass change in this phase is only $\delta M/M = t_{up}/t_S \sim 0.02\,\epsilon_{0.1}$, where the "Salpeter time" t_S (for an accreting black hole to e–fold in mass) is

$$t_S = M/\dot{M} = 4 \times 10^7\, \epsilon_{0.1}\,\text{yr}, \tag{5}$$

where we have parameterized the radiative efficiency in terms of $\epsilon_{0.1} = \epsilon/0.1$ because popular geometrically–thin optically–thick accretion disk models rarely exceed efficiencies of $\epsilon_{0.1} = 1$.

This leads to the disturbing conclusion that QSOs accrete only a tiny fraction of their mass while in their bright phase. This result, which depends critically on comparing the upper end of the AGN luminosity function with the upper end of the present–day MBH mass spectrum, is in sharp contrast with the near equality of the integral quantities (see Figure 1 & eqn 3): the total AGN background is roughly consistent with the total mass density in present–day MBHs, underpredicting the latter by a modest factor of 5 (consistent with significant accretion occurring as an advection dominated flow [54]). Since this integral constraint is dominated by bright objects, this conflict probably reflects a misidentification of the current fossil masses of the bright quasars.

A plausible explanation is that MBHs may *not* have stayed constant in mass from the QSO era until now, but rather grew in mass by an average factor F. This growth might occur because hierarchical clustering merged these MBH's along with their protogalaxies. These mergers need not emit light. In that case, luminous quasars should be identified with MBHs today that are larger by the factor F, and their spheroids would be brighter by nearly the same factor. The exponential cutoff in the bright end of the luminosity function makes such spheroids much rarer and closer in abundance to the space density of QSOs.

Specifically, for $F = 5$ the limiting MBH mass today becomes $2\times10^9\, M_\odot$, the limiting spheroid luminosity is $4 \times 10^{10}\, L_\odot$, and the new benchmark galaxy in the luminosity function has $M_B = -22.2$, which is 300 times rarer. The difference in space density between quasars and spheroids is reduced to a factor of 3, the duty cycle comes up to 1/3, and the lifetime of the bright phase is $\sim 3 \times 10^8$ yr. In this model bright quasars now spend a few Salpeter lifetimes in the bright phase, which is more plausible.

Is growth by a factor $F \sim 5$ reasonable? Data on the recently discovered Lyman–Break Galaxies (LBGs) indicate slightly more growth. LBGs have been suggested by several authors as the early–formation phase of spheroidal components [55, 56, 57]. Small radii ($1 - 2$kpc [58, 56]) and small velocity dispersions (measured for only a handful of the brightest objects [59]) indicate modest masses of order a few $\times10^9\, M_\odot$. If these merge to form typical spheroids of today with $L \sim 10^{10}\, L_\odot$ and masses $M \sim 5 \times 10^{10}\, M_\odot$, growth by more like a factor of 10 would be required. Models of hierarchically clustering protogalaxies [60] also suggest growth by $F \sim 10$.

A second item that favors more growth is the lack of detection of AGNs in LBGs. If MBHs are forming everywhere in protogalaxies together with stars at the universal ratio $M_\bullet/M_{star} = 0.005$ (Figure 1), then the average bright LBG should contain an MBH of about $10^7\, M_\odot$, with Eddington luminosity $L_E \sim 10^{45}$ ergs/sec. The apparent magnitude of such an object at $z = 3$ (including absorption by the factor 3–10 that affects LBGs [61]) is about $m_B = 26 - 27$, arguably faint enough to have escaped spectroscopic detection so far.

4.2 The Era of Galaxies

If both MBHs and mergers are common among spheroids, two galaxies with pre–existing MBHs will frequently merge. The MBHs will spiral towards the center of the merger remnant, heating and perhaps ejecting stars from the center [1]. It is observed [62] that low–luminosity ellipticals and spiral bulges possess steeply rising central star profiles that approximate power laws, while high–luminosity ellipticals have central profiles that turn over to form much less dense centers (termed "cores"). The dense power–law centers of the small spheroids, their disky isophotes, and rapid rotation suggest that gas–rich, dissipative mergers or collapse may have controlled their mass distributions [63, 64, 65], perhaps in the presence of one or more MBHs.

The formation of the low–density cores of luminous core galaxies is more difficult. Cosmological simulations tend to produce dark matter distributions with dense centers [66], and dissipation is likely to sharpen their centers as would adiabatic compression by accretion of mass by a central black hole. [67, 65] In the *dissipationless* merger of gas–poor galaxies, the orbits of the associated MBHs would scour out a core in the stellar mass distribution, with a mass that tracks the black hole mass [67]. The predicted core masses and radii are a fair match to those observed, assuming that each spheroid has a BH given by the standard mass ratio $M_\bullet/M_{star} = 0.005$ [65]. The dissipationless mergers envisioned here are consistent with other characteristics of core galaxies such as their low rotation and boxy isophotes. An additional virtue of MBHs in core galaxies is that they may protect the cores from infilling by accreting low–mass, high–density satellites (by tidally shredding them), which may otherwise give luminous galaxies very bright centers.

5 Tests of the Picture

The detection of supermassive black holes and the discovery of dark matter share a common feature. In both cases there was skepticism of dynamical mass measurements, and acceptance was preceded by decades of debate. Dark matter has since come to be an essential feature of our understanding of many phenomena, ranging from galaxy rotation curves to the formation of structure in the Universe. We now seem engaged in a similar transition in the prevailing view of the centers of galaxies.

An inevitable source of fuel for dead quasar engines is the debris from tidally disrupted stars. MBHs with masses $M_\bullet \lesssim 10^8 M_\odot$ disrupt main–sequence stars rather than swallowing them whole. Some of the debris from the star is ejected, but a portion remains bound to the MBH, forming an accretion disk that undergoes a "flare" lasting a few months to a year [28, 68]. Plausible models [69] predict a V–band luminosity of about $10^9 L_\odot$. The event rate is controlled by how quickly stars can drift into the "loss cone" of low–angular–momentum orbits that come close to the MBH. Calculations show that faint, compact galaxies (e.g., M32) have the highest disruption rates, about $10^{-4}\mathrm{yr}^{-1}$. Larger, more diffuse galaxies (e.g., M87) have much lower rates of about $10^{-6}\mathrm{yr}^{-1}$, and often have sufficiently massive black holes to consume main sequence stars whole. It is possible that a stellar disruption by an MBH has already been witnessed spectroscopically. The nucleus of the spiral galaxy NGC 1097 exhibited an ephemeral, broad, double–peaked Hα emission line [70], whose profile matched that expected from an accretion disk [71].

Finally, it may be possible to detect the gravitational wave signature of merging MBHs, and thereby constrain the merger history of galaxies. In hierarchical models a typical bright galaxy has merged a few times since the quasar era. The timescales for decay of binary black holes in different regimes indicate that, for MBH with $M_\bullet \gtrsim 10^7 M_\odot$, the binary holes will merge on a timescale short compared to the next merger time [72]. The merger rate for galaxies above $0.01L^*$ may exceed 1/yr in the visible Universe. For an equal–mass binary black hole, the final orbit produces a luminosity of order $L_{grav} \sim c^5/G = 10^{60}$ergs/sec in gravitational radiation, independent of $M_\bullet$. These mergers are the most powerful events in the Universe, but ironically they may not produce electromagnetic radiation. The energy is emitted over a time $t \propto GM_\bullet/c^3$. The distinctive signature of a supermassive MBH merger as opposed to two stellar–mass black holes is the lower frequency and longer duration. Two $10^7 M_\odot$ black holes radiate much of their energy at a frequency about 10^{-4} Hz. These events are too slow for LIGO (the Laser Interferometry Gravitational-wave Observatory, but are easy for LISA (the Laser Interferometric Space Array proposed as a Cornerstone Mission for ESA). A key test of the ideas in this paper is the observation of gravitational radiation from merging black holes at the centers of merged galaxies since $z \sim 3$.

References

[1] Begelman, M. C. & Rees, M. J. Gravity's Fatal Attraction, (W. H. Freeman & Co., NY 1996).

[2] Kormendy, J. & Richstone, D. Inward bound — the search for massive black holes in galactic nuclei. *Ann. Rev. Astron. & Astroph.* **33,** 581 — 624 (1995).

[3] Kafatos, M. (ed.) "Supermassive Black Holes", (Cambridge U Press, Cambridge 1988).

[4] Barr, P. & Mushotzky, R. F. Limits of X-ray variability in active galactic nuclei. *Nature* **320**, 421 — 423 (1986).

[5] Edelson, R. *et al.* Multiwavelength observations of short–timescale variability in NGC 4151. IV. Analysis of multiwavelength continuum variability. *Astrophys. J.* **470,** 364 — 377 (1996).

[6] Lynden-Bell, D. Galactic nuclei as collapsed old quasars. *Nature* **223,** 690 — 694 (1969).

[7] Blandford, R. D. Physical process in active galactic nuclei. in Active Galactic Nuclei (ed. Blandford, R. D., Netzer, H. & Woltjer, L.) (Springer-Verlag, Berlin 1990), pp 161 –274.

[8] Abramowicz, M. A., Bjornsson, G. & Pringle, J. E. The Theory of Black Hole Accretion Discs (Cambridge University Press, Cambridge 1998).

[9] Bahcall, J. N., Kirhakos, S., Saxe, D. H. & Schneider, D. P. Hubble space telescope images of a sample of 20 nearby luminous quasars. *Astrophys. J.* **479,** 642 - 658 (1997).

[10] Zeldovich, Ya. B. & Novikov, I. D. An estimate of the mass of a superstar. Doklady Akad. Nauk. SSSR 164, **158,** 311 — 315 (1964).

[11] Salpeter, E. E., Accretion of interstellar matter by massive objects. *Astrophys. J.* **140,** 796 — 799 (1964).

[12] Lynden-Bell, D. Gravity Power. Physica Scripta **17,** 185 — 191 (1978).

[13] Chokshi A. and Turner, E. L. Remnants of the quasars. *Mon. Not. R. Astr. Soc.* **259,** 421 — 424 (1992).

[14] Loveday, J., Peterson, B. A., Efstathiou, G. and Maddox, S. J. The Stromlo–APM redshift survey. I. The luminosity function and space density of galaxies. *Astrophys. J.* **390,** 338 — 344 (1992).

[15] Sargent, W. L. W. *et al.* Dynamical evidence for a central mass concentration in the galaxy M87. *Astrophys. J.* **221,** 731 — 744 (1978).

[16] Dressler, A. & Richstone, D. O. Stellar dynamics in the nuclei of M31 and M32: evidence for massive black holes. *Astrophys. J.* **324,** 701 — 713 (1988).

[17] Kormendy, J. Evidence for a supermassive black hole in the nucleus of M31. *Astrophys. J.* **325,** 128 — 141 (1988).

[18] Schwarzschild, M. A dynamical model for a triaxial stellar system in dynamical equilibrium. *Astrophys. J.* **232,** 236 — 247 (1979).

[19] Richstone, D. O. & Tremaine, S. Maximum entropy models of galaxies. *Astrophys. J.* **327,** 82 — 88 (1988).

[20] Harms, R. *et al.* HST FOS spectroscopy of M87: evidence for a disk of ionized gas and a massive black hole. *Astrophys. J. Letters.* **435**, L35 —L38 (1994).

[21] Ford, H. C. *et al.* Narrowband HST images of M87: evidence for a disk of ionized gas and a massive black hole. *Astrophys. J. Letters.* **435,** L27 — L30 (1994).

[22] The supermassive black hole of M87 and the kinematics of its associated gaseous disk. Macchetto, F. *et al.* *Astrophys. J.* **489**, 579 — 600 (1997).

[23] Young, P. J., Westphal, J. A., Kristian, J., Wilson, C. P. & Landauer, F. P. Evidence for a supermassive object in the nucleus of the galaxy M87 from SIT and CCD area photometry. *Astrophys. J.* **221,** 721 — 730 (1978).

[24] Miyoshi, M. *et al.* Evidence for a black hole from high rotation velocities in a sub–parsec region of NGC 4258. *Nature* **373**, 127 — 129 (1995).

[25] Maoz, E. A stringent constraint on alternatives to a massive black hole at the center of NGC 4258. *Astrophys. J. Letters.* **447**, L91 — L94 (1995). Updated in Maoz, E. Dynamical constraints on alternatives to supermassive black holes in galactic nuclei. *Astrophys. J. Letters.* **491**, L181 — 184 (1998).

[26] Genzel, R. & Eckart, A. A massive black hole at the center of the Milky Way. C. R. Acad. Sci. Paris, **326,** Serie II b, 69 — 78 (1998). Also, Genzel, R. Eckart, A. Ott, T. & Eisenhauer, F. On the nature of the dark mass in the centre of the Milky Way. *Mon. Not. R. Astr. Soc.* **291,** 219 — 234 (1997).

[27] Ghez, A. M., Klein, B. L., Mccabe C., Morris, M., & Becklin, E. E. High proper motions in the vicinity of SGR A*. in the Proceedings of IAU Symposium 184, Kyoto, The Central Region of the Galaxy and Galaxies (ed. Y. Sofue) Kluwer, Dordrecht (1998).

[28] Goodman, J. & Lee, H.-M. Black holes or dark clusters in M31 and M32? *Astrophys. J.* **337**, 84 — 90 (1989).

[29] Netzer, H. & Peterson, B. M. 1997, in Astronomical Time Series, ed. D. Maoz, A. Sternberg & E. M. Leibowitz (Dordrecht: Kluwer), 85 — 108

[30] Ho, L. C. "Supermassive Black Holes in Galactic Nuclei: Observational Evidence and Some Astrophysical Consequences." In *Observational Evidence for Black Holes in the Universe*, ed. S. K. Chakrabarti (Dordrecht: Kluwer), 157 – 187 (1998).

[31] Kaspi, S. *et al.* Multiwavelength observations of short – timescale variability in NGC 4151. II. Optical observations. *Astrophys. J.* **470**, 336 — 348 (1996).

[32] Tanaka, Y. *et al.* Gravitationally redshifted emission implying an accretion disk and massive black hole in the active galaxy MCG-6-30-15. *Nature* **375**, 659 — 661 (1995).

[33] Nandra, K., George, I. M., Mushotzky, R. F., Turner, T. J. & Yaqoob, T. ASCA observations of Seyfert 1 galaxies. II. Relativistic Iron Kα emission. *Astrophys. J.* **477**, 602 — 622 (1997).

[34] Reynolds, C. S. & Begelman, M. C. Iron fluorescence from within the innermost stable orbit of black hole accretion disks. *Astrophys. J.* **488**, 109 — 118 (1997).

[35] Bromley, B. C., Miller, W. A. & Pariev, V. I. The inner edge of the accretion disk around a supermassive black hole. *Nature* **391**, 54 — 56 (1998).

[36] Kormendy, J. in The Nearest Active Galaxies, ed. J. Beckman, L. Colina & H. Netzer (Madrid: Consejo Superior de Investigaciones Científicas) 197 — 218 (1993).

[37] Magorrian J. *et al.* The demography of massive dark objects in galaxy centers. *Astron. J.* **115**, in press (1998).

[38] Ho, L.C., Filippenko, A.V. & Sargent, W.L.W. A search for "dwarf" Seyfert nuclei. V. Demographics of nuclear activity in nearby galaxies. *Astrophys. J.* **487**, 568 — 578 (1997).

[39] Moran, E. C. *et al.* X-Rays from NGC 4395, the least luminous Seyfert 1 nucleus. Submitted to *Astrophys. J.*

[40] de Blok, W.J.G., McGaugh, S.S. & van der Hulst, J.M. HI observations of low surface brightness galaxies: probing low-density galaxies. *Mon. Not. R. Astr. Soc.* **283**, 18 — 54 (1996).

[41] Madau, P., Ferguson, H. C., Dickinson, M. E., Giavalisco, M., Steidel, C. C. & Fruchter, A. High-redshift galaxies in the Hubble Deep Field: Colour selection and star formation history to $z \sim 4$. *Mon. Not. R. Astr. Soc.* **283**, 1388 — 1404 (1996).

[42] Connolly, A. J., Szalay, A. S. Dickinson, M., Subbarao, M. U. & Brunner, R. J. The evolution of the global star formation history as measured from the Hubble Deep Field. *Astrophys. J. Letters.* **486**, L11 — L14 (1997).

[43] Pettini, M., Steidel, C.C., Adelberger, K.L., Kellogg, M., Dickinson, M. & Giavalisco, M. in "Cosmic Origins: Evolution of Galaxies, Stars, Planets and Life" ed. J.M. Shull, C.E. Woodward, and H.A. Thronson, (ASP Conference Series), in press (1998).

[44] Schmidt, M., Schneider, D. P. & Gunn, J. E. Spectroscopic CCD surveys for quasars at large redshift. IV. Evolution of the luminosity function from quasars detected by their Lyman-alpha emission. *Astron. J.* **110,** 68 — 77 (1995).

[45] Boyle, B. J., Terlevich, R. J. The cosmological evolution of the QSO luminosity density and of the star formation rate. *Mon. Not. R. Astr. Soc.* **293**, L49 — L51 (1998).

[46] Haehnelt, M. G. and Rees, M. J. The formation of nuclei in newly formed galaxies and the evolution of the quasar population. *Mon. Not. R. Astr. Soc.* **263**, 168 — 178 (1993). See also Haehnelt, M. G., Natarajan, P. & Rees, M. J. High-redshift galaxies, their active nuclei and central black holes. Submitted to *Mon. Not. R. Astr. Soc.* (1997).

[47] Blumenthal, G.R., Faber, S.M., Primack, J.R., Rees, M.J. Formation of galaxies and large-scale structure with cold dark matter. *Nature* **311**, 517 — 525 (1984).

[48] Merritt, D. & Quinlan, J. D. Dynamical evolution of elliptcal galaxies with central singularities. *Astrophys. J.* **498**, 625 – 639 (1998)

[49] Sellwood, J. A. & Moore, E. M. On the formation of disk galaxies and massive central objects. *Astrophys. J.* submitted (1998).

[50] Boyle, B.J., Jones, L.R., Shanks, T., Marano, B., Zitelli, V. & Zamorani, G. "QSO evolution and clustering at $z < 2.9$" in The Space Distribution of Quasars (ed D. Crampton) pp. 191 — 198 (San Francisco: Astron. Soc. Pac, 1991). See also Boyle, B. J. Shanks, T. & Peterson, B. A. The Evolution of Optically Selected QSOs – II. *Mon. Not. R. Astr. Soc.* **235**, 935 — 948 (1988).

[51] Sanders, D. B., Phinney, E. S., Neugebauer, G., Soifer, B. T. & Matthews, K. Continuum energy distributions of quasars: shapes and origins. *Astrophys. J.* **347**, 29 — 51 (1989).

[52] Simien, F. & de Vaucouleurs, G. Systematics of bulge-to-disk ratios. *Astrophys. J.* **302**, 564 — 578 (1986).

[53] Binggeli, B., Sandage, A. & Tammann, G. A. The luminosity functions of galaxies. *Ann. Rev. Astron. & Astroph.* **26**, 509 — 560 (1988).

[54] Narayan, R., Mahadevan, R., and Quataert, E. in "The Theory of Black Hole Accretion Discs", eds Abramowicz, Bjornsen & Pringle (Cambridge U Press) 1988, and also astro-ph/9803141.

[55] Steidel, C. C., Giavalisco, M., Pettini, M., Dickinson, M. & Adelberger, K. L. Spectrosopic confirmation of a population of normal star-forming galaxies at redshifts $z > 3$. *Astrophys. J. Letters.* **462**, L17 — L21 (1996).

[56] Lowenthal, J.D. *et al.* Keck spectroscopy of redshift $z \sim 3$ galaxies in the Hubble deep field. *Astrophys. J.* **481**, 673 — 688 (1997).

[57] Trager, S.C., Faber, S.M., Dressler, A. & Oemler, A. Galaxies at $z \approx 4$ and the formation of Population II. *Astrophys. J.* **485**, 92 — 99 (1997).

[58] Giavalisco, M., Steidel, C.C. & Machetto, F.D. Hubble Space Telescope imaging of star-forming galaxies at redshifts $z > 3$. *Astrophys. J.* **470**, 189 — 194 (1996).

[59] Pettini, M. *et al.* . Infrared observations of nebular emission lines from galaxies at z=3. *Astrophys. J.* in the press (1998).

[60] Somerville, R., Primack, J. & Faber, S.M. The nature of high redshift galaxies. *Astrophys. J.* submitted (1998).

[61] Meurer, G., Heckman, T., Lehnert, M., Leitherer, C. & Lowenthal, J. The panchromatic starburst intensity limit at low and high redshift. *Astron. J.* **114**, 54 — 68 (1997).

[62] Lauer, T.R. *et al.* The centers of early-type galaxies with HST. I. An observational survey. *Astron. J.* **110**, 2622 — 2654 (1995).

[63] Nieto, J.-L., Bender, R. & Surma, P. Central brightness profiles and isophotal shapes in elliptical galaxies. *Astron. Astroph.* **244**, L37-L40 (1991).

[64] Bender, R., Burstein., D. & Faber, S.M. Dynamically hot galaxies. I – Structural properties. *Astrophys. J.* **399**, 462 — 477 (1992).

[65] Faber, S.M. *et al.* The centers of early-type galaxies with HST. IV. Central parameter relations. *Astron. J.* **114**, 1771 — 1796 (1997).

[66] Navarro, J.F., Frenk, C. & White, S.D.M. The structure of Cold Dark Matter halos. *Astrophys. J.* **462**, 563 — 575 (1996).

[67] Quinlan, G.D. The dynamical evolution of massive black hole binaries I. Hardening in a fixed stellar background. *New Astronomy* **1**, 35 — 56 (1996).

Quinlan, G.D. & Hernquist, L. The dynamical evolution of massive black hole binaries II. Self-consistent N-body integrations. *New Astronomy* **2**, 533 — 554 (1997).

[68] Rees M.J., Tidal disruption of stars by black holes of $10^6 - 10^8$ solar masses in nearby galaxies. *Nature* **333**, 523 — 528 (1988).

[69] Ulmer, A. Flares from the tidal disruption of stars by massive black holes. *Astrophys. J.* , in press (1998).

[70] Storchi-Bergmann, T. *et al.* The variability of the double-peaked Balmer lines in the active nucleus of NGC 1097. *Astrophys. J.* **443**, 617 — 624 (1995).

[71] Chen, K. & Halpern, J. P. Structure of line-emitting accretion disks in active galactic nuclei – Arp 102B. *Astrophys. J.* **344**, 115 — 124 (1989).

[72] Xu, G. & Ostriker, J. P. Dynamics of massive black holes as a possible candidate of Galactic dark matter. *Astrophys. J.* **437**, 184 — 193 (1994).

[73] Tonry, J. Evidence for a central mass concentration in M32. *Astrophys. J. Letters.* **283**, L27–L30 (1984).

[74] Bender, R., Kormendy, J. & Dehnen, W. Improved evidence for a $3 \times 10^6 M_\odot$ Black Hole in M32 *Astrophys. J. Letters.* 464, L123-L126 (1996).

[75] van der Marel, R. P., Cretton, N., de Zeeuw, P. T. & Rix, H.-W. Improved evidence for a black hole in M32 from HST/FOS spectra. II. Axisymmetric dynamcial models. *Astrophys. J.* **493,** 613-631 (1998).

[76] Kormendy, J. & Richstone, D. Evidence for a supermassive black hole in NGC 3115. *Astrophys. J.* **393**, 559 — 578 (1992).

[77] Kormendy, J. *et al.* Hubble Space Telescope spectroscopic evidence for a $2 \times 10^9\, M_\odot$ black hole in NGC 3115. *Astrophys. J. Letters.* **459**, L57 — L60 (1996).

[78] Kormendy, J., Bender, R., Evans, A. & Richstone, D. The mass distribution in the elliptical galaxy NGC 3377: evidence for a $2 \times 10^8\, M_\odot$ Black Hole. *Astron. J.* **115**, 1823 — 1839 (1998).

[79] Gebhardt, K. *et al.* Axisymmetric, three-integral models of galaxies: A massive black hole in NGC 3379. *Astrophys. J.* submitted (1988).

[80] Cretton, N. & van den Bosch, F. C. Evidence for a massive black hole in the S0 galaxy NGC 4342. Submitted to *Astrophys. J.* (1998). astro-ph/9805324.

[81] Kormendy, J. *et al.* Hubble Space Telescope spectroscopic evidence for a $1 \times 10^9\, M_\odot$ black hole in NGC 4594. *Astrophys. J. Letters.* **473**, L91 — L94 (1996).

[82] Kormendy, J. Evidence for a central dark mass in NGC 4594 (the Sombrero galaxy). *Astrophys. J.* **335**, 40 — 56 (1988).

[83] Bower, G. A. *et al.* Kinematics of the nuclear ionized gas in the radio galaxy M84 (NGC 4374). *Astrophys. J. Letters.* **492**, L111 — L114 (1998).

[84] Ferrarese, L., Ford, H. C. & Jaffe, W. Evidence for a massive black hole in the active galaxy NGC 4261 from Hubble Space Telescope images and spectra. *Astrophys. J.* **470**, 444 — 459 (1996).

[85] van der Marel, R. P. & van den Bosch, F. C. Evidence for a 3×10^8 solar mass black hole in NGC 7052 from HST observations of the nuclear gas disk. *Astron. J.* submitted (1998). Astro-ph/9804194

[86] Greenhill, L. J., Gwinn, C. R., Antonucci, R. & Barvainis, R. VLBI imaging of water maser emission from the nuclear torus of NGC 1068. *Astrophys. J. Letters.* **472**, L21 — L24 (1996).

[87] Greenhill, L. J., Moran, J. M. & Herrnstein, J. R. The distribution of H_2O maser emission in the Nucleus of NGC 4945. *Astrophys. J. Letters.* **481**, L23 — L26 (1997).

[88] Jones, D. *et al.* Visible and far-ultraviolet WFPC2 imaging of the nucleus of the galaxy NGC 205. *Astrophys. J.* **466**, 742 — 749 (1996).

[89] Kormendy, J. & McClure, R. D. The nucleus of M33. *Astron. J.* **105**, 1793 — 1812 (1993).

We thank Sofia Kirhakos for providing images of quasar host galaxies from reference [9], and Pawan Kumar and John Bahcall for useful discussions. We thank Carl Grillmair for years of fruitful discussions. Much of this article depends on research done with the Hubble Space Telescope. We have enjoyed considerable financial support from NASA. DR acknowledges the generous support of the J. S. Guggenheim Foundation and the Ambrose Monell Foundation while at the IAS.

Author Affiliations: D. Richstone, Dept of Astronomy, Univ of Michigan **dor@umich.edu**; E. A. Ajhar, NOAO; R. Bender, Ludwig–Maximilians University, Munich; G. Bower, NOAO; A. Dressler, Observatories of the Carnegie Institution of Washington; S. M. Faber, Lick Observatory, University of California; A. V. Filippenko, Dept. of Astronomy, U. C. Berkeley; K. Gebhardt, Lick Observatory, University of California; R. Green, NOAO; L. C. Ho, Harvard–Smithsonian Center for Astrophysics; J. Kormendy, Institute of Astronomy, Univ of Hawaii; T. Lauer, NOAO; J. Magorrian, Canadian Institute of Theoretical Astronomy; S. Tremaine, Dept. of Astrophysical Sciences, Princeton U.